MNRAS 000, 1–7 (2017) Preprint 20 April 2022 Compiled using MNRAS LATEX style file v3.0

Does Fornax have a cored halo? Implications for the nature of dark matter

Pierre Boldrini[1]★, Roya Mohayaee[1], Joseph Silk[1,2,3]
[1]Sorbonne Université, CNRS, UMR 7095, Institut d'Astrophysique de Paris, 98 bis bd Arago, 75014 Paris, France
[2]Department of Physics and Astronomy, The Johns Hopkins University, Baltimore MD 21218, USA
[3]Beecroft Institute for Particle Astrophysics and Cosmology, Department of Physics, University of Oxford, Oxford OX1 3RH, UK

Last updated 2018 June 12; in original form xxxxxxx

ABSTRACT

Fornax is the most massive of the Milky Way dwarf spheroidal galaxies and has five globular clusters orbiting in a dense background of dark matter. Observational analyses suggest that globular clusters were initially much more massive and lost most of their stars to the Fornax field. We re-investigate the Fornax cusp-core problem, to clarify tensions between simulations and observations concerning the dark matter halo density profile. N-body simulations predict a centrally steep power-law density profile, while observations of the globular clusters seem to prefer that the dark matter halo density is constant at the center. For the first time, we ran pure N-body simulations with entirely live systems, i.e. self-gravitating systems composed of particles (including stars and dark matter). Only this numerical approach accounts correctly for dynamical friction and tidal effects between Fornax and the globular clusters. We show that a weak cusp (r_s = 1.5 kpc) or a large core (r_c = 848 pc) are not compatible with the current observed positions and masses of Fornax clusters. In contrast, a small dark matter core (r_c = 282 pc) for Fornax naturally reproduces the cluster spatial and mass distributions over a wide range of initial globular cluster masses. We derive an upper limit of $r_c \lesssim 282$ pc. This core size range favors only warm dark datter (WDM). It is also possible to obtain a compatible core size range from cold dark matter (CDM) theories, if the initial halo's central cusp is heated by gas to form a small core.

Key words: stellar dynamics - methods: N-body simulations - galaxies: kinematics and dynamics - galaxies: structure - galaxies: halos

1 INTRODUCTION

Cold dark matter (CDM) cosmology is the standard paradigm of structure formation in the Universe. However, there are a few unresolved issues on small scales in the context of this model such as the missing satellites problem, the too-big-to-fail problem, the cusp-core problem and the satellite disk problem (see e.g. Bullock & Boylan-Kolchin (2017) for a recent work). We focus here on the cusp-core problem. Observations of dwarf galaxies have revealed that the density profile of the dark matter (DM) halo is constant at the center of dwarf galaxies (Moore 1994; Burkert 1995; de Blok et al. 2001; Swaters et al. 2003; Spekkens et al. 2005). In contrast, N-body simulations have generally predicted a steep power-law mass-density distribution at the center of CDM halos (Navarro et al. 1997; Fukushige & Makino 1997; Moore et al. 1998). Resolving the cusp-core problem could provide important evidence for the nature of dark matter, e.g. to help distinguish between cold dark matter (CDM), warm dark matter (WDM) (Dolgov & Hansen 2002), fuzzy dark matter (FDM) (Hu et al. 2000; Hui et al. 2017) and self-interacting dark matter (SIDM) (Spergel & Steinhardt 2000). These theories are often motivated via the need for resolution of the cusp-core problem.

Dwarf spheroidal (dSphs) galaxies are the most dark matter-dominated galaxies in the Universe (Mateo (1998) and references therein). In some dSphs, dark matter contributes 90% or more of the total mass, even at the center of the galaxy, so the dynamics is determined entirely by the gravitational field of the dark matter. Therefore, these systems provide an excellent laboratory to study dark matter in the context of galaxy formation and evolution. Fornax is the most massive of the Milky Way dSphs and is the only one to have five globular clusters orbiting in a dense background of dark matter. For instance, another major dSph, such as the Sagittarius dSph, has four globular clusters. The study of globular cluster dynamics can place powerful constraints on the Fornax dark matter halo type.

One apparent paradox about these clusters is that we don't expect to see any of them because they should have sunk to the center of Fornax due to dynamical friction (Chandrasekhar 1943). It is precisely because of this drag force that globular cluster are expected to sink to the center of their host galaxy (Binney & Tremaine 2008).

★ Contact e-mail: boldrini@iap.fr

Object	Mass $[10^5\ M_\odot]$	r_k [pc]	r_h [pc]	D_p [kpc]	Distance [kpc]
dSph	1420	668	-	-	147 ± 4
GC1	0.42 ± 0.10	10.03	20.4	1.6	147.2 ± 4.1
GC2	1.54 ± 0.28	5.81	11.82	1.05	143.2 ± 3.3
GC3	4.98 ± 0.84	3.54	7.2	0.43	141.9 ± 3.9
GC4	0.76 ± 0.15	2.41	4.9	0.24	140.6 ± 3.2
GC5	1.86 ± 0.24	4.18	8.5	1.43	144.5 ± 3.3

Table 1. Observed data for the Fornax system. r_k is the King radius for the globular clusters and the half-light radius for the dSph. r_h is the half-mass radius for the globular clusters. D_p is the projected distance of the globular cluster (GC) from the center of Fornax. The last column is the line-of-sight distance from us (de Boer & Fraser 2016; Cole et al. 2012; Larsen et al. 2012).

However, we are still observing globular clusters orbiting in Fornax. This has become known as the Fornax timing problem. Since dynamical friction force depends directly on the density of dark matter halo, the timing problem could be used to probe the cusp-core problem. Changing the density profile could delay dynamical friction. Simulations agree well with Chandrasekhar's analytic calculation for a cuspy halo such as Navarro-Frenk-White (NFW) halo, which is the most commonly used model for dark matter halos (Goerdt et al. 2006). Enhancement of the infall time can be achieved by changing the density profile of the dark matter halo.

Numerous simulations have been performed to study the timing problem, but they are oversimplified and do not capture all of the physics (Oh et al. 2000; Goerdt et al. 2006; Read et al. 2006; Cole et al. 2012). In these simulations, Fornax was modelled as a live galaxy, i.e. a self-gravitating system composed of star and dark matter particles. However, globular clusters are not modeled as live objects, but are only represented by point masses. Consequently, dynamical friction and tidal effects are not properly taken into account. Furthermore, these studies took into account only the tidal perturbation of Fornax due to the Milky Way, neglecting the tidal interactions between Fornax and the globular clusters. Goerdt et al. (2006) proposed that a cored dark matter halo provides a solution to the timing problem. In this model, globular clusters stop sinking at the core radius because of a prospective resonance/scattering effect. Later work provided further support for a large dark matter core for Fornax (Cole et al. 2012). The globular clusters did not fall to the center because of 'dynamical buoyancy' created by the Fornax core. They also proposed that globular clusters have not formed within Fornax, but they have been accreted by Fornax, which has a small cored halo.

Here, we re-investigate the Fornax cusp-core problem using N-body simulations with entirely live objects i.e. fully composed of particles, in order to take into account correctly dynamical friction and tidal effects between Fornax and its globular clusters. The paper is organized as follows. Section 2 is devoted to describe clearly the Fornax system and the N-body modeling. In Section 3, we present details of our numerical simulations. In Section 4, we present our results of simulations and discuss the implication of our result on the nature of dark matter.

2 FORNAX-GLOBULAR CLUSTER SYSTEM

The dSph galaxy Fornax is one of the most dark matter-rich satellites of the Milky Way with a mass of about 10^8 $M_\odot$ at a distance of about 147 kpc (de Boer & Fraser 2016). Fornax contains five globular clusters with masses of about 10^5 $M_\odot$ and the average projected distance of these clusters is about 1 kpc. Various details are given in Table 1.

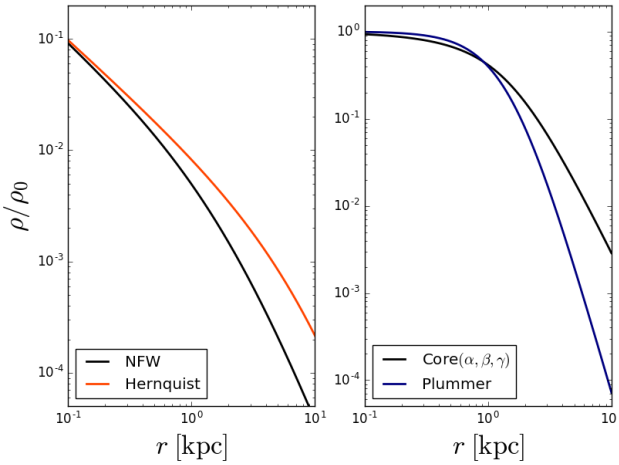

Figure 1. Analytic density profiles of NFW and Hernquist halos (*left panel*). The scale radius for NFW profile is $r_s = 2.4$ kpc and for Hernquist profile is $r_s = 1.5$ kpc. Analytic density profiles of core (α, β, γ) and Plummer halos (*right panel*). The scale radius for core profile is $r_s = 2.4$ kpc and for Plummer profile is $r_s = 1.5$ kpc. Since the globular cluster is initially placed at a radius of about 1.6-2 kpc, our results remain robust to divergences between different profiles at large scales.

In this section, we present the models for Fornax and its globular clusters that provide the initial conditions for our simulations.

2.1 Fornax modelling

We construct Fornax as a live galaxy composed of stars and a dark matter halo only, since dSph galaxies contain little or no gas. The Fornax star component is modeled due to the presence of the dSph core by a Plummer profile

$$\rho(r) = \frac{3r_s^2 M_0}{4\pi}(r^2 + r_s^2)^{-5/2}, \tag{1}$$

with $r_s = 668$ pc and $M_0 = 14.2 \times 10^7$ $M_\odot$. For the dark matter halo of Fornax, we use two different density profiles: one with the central cusp and one with a core. For cuspy simulation, we use the Hernquist profile

$$\rho(r) = \frac{M_0}{2\pi}\frac{r_s}{r(r+r_s)^3}, \tag{2}$$

with $r_s = 1.5$ kpc and $M_0 = 2 \times 10^9$ $M_\odot$. Unlike NFW profile, the Hernquist behaves as $1/r^4$ at large r. For cored simulation, we construct a Plummer profile (see equation (1)). For large r, the profile behaves as $1/r^5$ unlike the cored profile based on the α, β, γ law (Hernquist 1990) which behaves as $1/r^3$. At the r range relevant for this work ($r < 2$ kpc), the profiles agree closely as shown in Figure 1 (Springel et al. 2005). The halo of Fornax is represented by $N = 10^6$ particles while the star component has $N = 10^5$ particles in our simulation.

For the Fornax halo, we selected three models: WC (Weak Cusp), LC (Large Core) and SC (Small Core). WC and LC density profiles are based on models of Cole et al. (2012). We ran simulations with these three different halos. For LC and SC halos, the core is defined as the constant density region in our models and its radius is given by

$$\rho(r_c) = \frac{\rho_0}{2}, \tag{3}$$

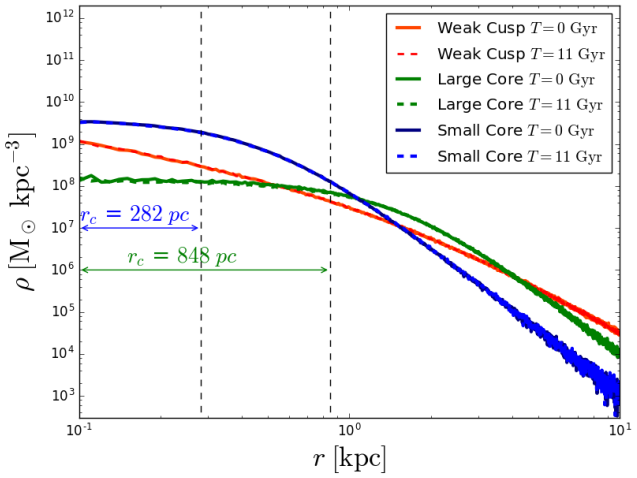

Figure 2. Density distributions of dark matter halos for Weak Cusp (orange line), Large Core (green line) and Small Core (blue line) models used in the numerical simulations at the beginning $T = 0$ Gyr (solid line) and at the end of the simulation $T = 11$ Gyr (dotted line). The radial density profiles of halos are unchanged over 11 Gyr. Core radii r_c are marked by a vertical dotted line. All halo parameters are summarized in Table 2.

where ρ_0 is the asymptotic density at the center of the halo. Plots of density profiles are given in Figure 2, where core radii r_c are marked by vertical dotted lines. In order to test halo stability during the simulation, the initial conditions are compared with the final state of the system (see Figure 2). We state that our halo profiles are stable because the radial density profiles at $T = 0$ Gyr (solid line) and at $T = 11$ Gyr (dotted line) are the same.

2.2 Globular cluster modelling

There are five surviving globular clusters orbiting in Fornax. These globular clusters are modeled by a Plummer density profile (see equation (1)). We supposed that globular clusters were initially on a circular orbit with an orbital velocity

$$V_c^2(r) = \frac{4\pi G}{r} \int_0^r \rho(u) u^2 du, \tag{4}$$

which depends on the density profile of Fornax $\rho(u)$. Our globular cluster is represented by $N = 10^4$ particles. We chose a larger half-mass radius $r_h = 21$ pc than the observed radius, because it is susceptible to decrease through dynamical processes such as mass loss. It corresponds to a scale radius $r_s = 16$ pc. All data for Fornax-globular cluster system are summarized in Table 2.

The system is isolated in simulations because we neglect the Galactic tidal effects on Fornax-globular cluster system. Walker & Peñarrubia (2011) predicted the Fornax tidal radius $r_t \gtrsim 2$ kpc. Inside this radius, we can expect that tidal effects do not profoundly alter the structure and kinematics of Fornax.

To generate the initial conditions, we use the numerical code, NBODYGEN (Sadoun et al. 2014). This C++ code draws positions and velocities of each particles such that the resulting distribution follows the desired density profile $\rho(r)$. The code ensures that the final realization of the galaxy is in dynamical equilibrium.

Object	Density profile	r_s [kpc]	M_0 [M$_\odot$]	N
Star component	Plummer	0.514	14.2×10^7	10^5
Weak Cusp(WC)	Hernquist	1.5	2×10^9	10^6
Large Core(LC)	Plummer	1.5	2×10^9	10^6
Small Core(SC)	Plummer	0.5	2×10^9	10^6
Globular cluster(GC)	Plummer	0.016	-	10^4

Table 2. Data for Fornax-globular cluster system. r_s is the scale radius in density profiles. M_0 is the initial mass of the objects. The particle number is N. For the Fornax halo, we selected three models: WC (Weak Cusp), LC (Large Core) and SC (Small Core). WC and LC density profiles are based on models of Cole et al. (2012). For the globular cluster, we choose a larger half-mass radius r_h than the observed radius, because we expect that it will decrease through mass loss. It corresponds to a scale radius $r_s = 16$ pc.

3 N-BODY SIMULATIONS

Fornax is dominated by metal rich stars whereas globular cluster is dominated by metal-poor stars. If we compare the total mass of metal-poor ([Fe/H]<-2) cluster of $(8.81 \pm 0.92) \times 10^5 M_\odot$ to the metal-poor stellar mass in Fornax of $(44.9 \pm 5.3) \times 10^5$ $M_\odot$, this gives you a mass fraction of 19.6 ± 3.1 %, which means that a large fraction of the metal-poor stars in Fornax still belong to the globular clusters (de Boer & Fraser 2016). GC4 was excluded from this estimation, because this cluster is possibly more metal-rich than the other clusters. This high mass fraction, 19.6 ± 3.1 %, suggests that each of these four surviving metal-poor globular cluster has likely lost several times 10^5 $M_\odot$ due to dynamical processes such as dynamical friction, tidal effects and evaporation as a result of two-body relaxation. These processes act to destroy globular clusters on Gyr time-scales (Fall & Zhang 2001; Jordán et al. 2007). Thus, we supposed that globular clusters were initially much more massive in the past and lost most of their metal-poor stars to the Fornax field. We ran simulations for these previous halo models with a single globular cluster with initial masses $M_{GC_{ini}}$ of 1.71, 3.47 and 8.67 $\times 10^5 M_\odot$. Since the globular cluster mass is negligible as compared to Fornax, a single globular cluster should be sufficient for the study of the cusp-core problem.

The projected distances for the globular clusters are from 0.24 to 1.6 kpc, which is the minimum distance between globular cluster and the Fornax center. According to Figure 3, the radial distance can be greater than the projected distance. However, we suppose in our scenario that the globular clusters belong to Fornax. Thus, the globular cluster has to be close to the approximate Fornax tidal radius, which is about 2 kpc. We ran simulations with a globular cluster placed initially at a radius of 1.6 kpc and 2 kpc. To determine the globular cluster radial distance at each snapshot, we calculated the distance between the cluster mass center and Fornax mass center.

We performed our simulations with the N-body code, GADGET2 (Springel (2005)). We create, for each Fornax mass model, initial conditions for the Fornax-globular cluster system and evolve them for 10-11 Gyr because the Fornax globular cluster are all dominated by ancient (>10 Gyr) populations of stars (de Boer & Fraser 2016).

The gravitational softening parameter is set as 10 % of the globular cluster scale radius. Thus, the forces between all particles are softened with the same softening length $\epsilon = 1$ pc.

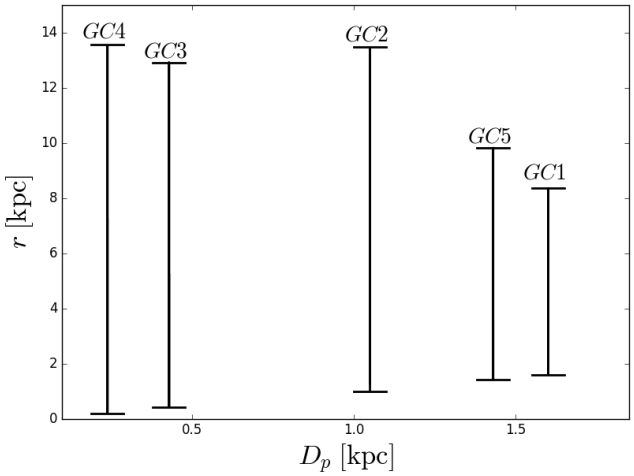

Figure 3. All possible radial distances from the center of Fornax for all the globular clusters, based on the observed line-of sight distance with uncertainties, as a function of the projected distance. The minimal values correspond to the current projected distance D_p of each globular cluster. The radial distance can be much bigger than the projected distance. However, we suppose in our scenario that the globular clusters belong to Fornax. Thus, the globular clusters have to be close to the approximate Fornax tidal radius, which is about 2 kpc. All observed data for globular clusters are summarized in Table 1.

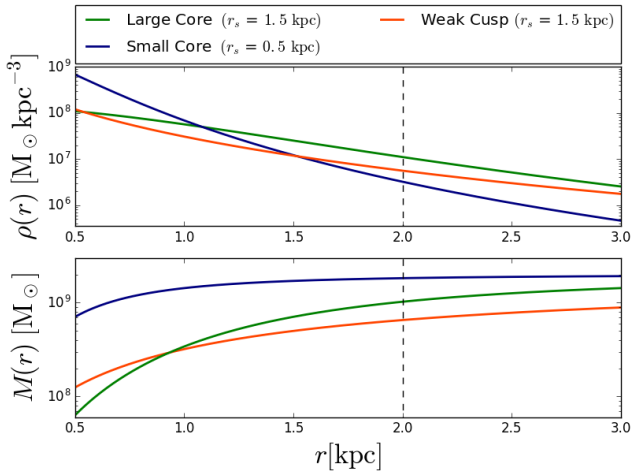

Figure 4. Density (*top panel*) and mass profiles (*bottom panel*) for three halo models. For both panels, the dashed lines correspond to the initial cluster radial distance r_i = 2 kpc. All halo parameters are summarized in Table 2.

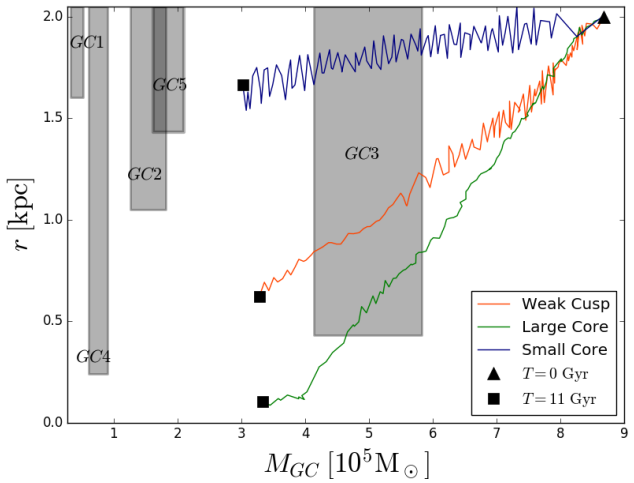

Figure 5. Globular cluster orbital decay as a function of mass loss with high initial mass $M_i = 8.67 \times 10^5$ M$_\odot$ and a globular cluster placed at r_i = 2 kpc from the center for the three halo models (Weak cusp, Large Core and Small Core). All halo parameters are summarized in Table 2. The black triangle (squares) corresponds to the initial T = 0 Gyr (final T = 11 Gyr) state. Final states compatible with observations, i.e. projected distance and globular cluster mass with their uncertainties, are represented by a grey area for each globular cluster. Observed data for globular clusters are summarized in Table 1.

4 RESULTS

We present and discuss our simulation results. To analyze our data and extract our results, we use a PYTHON module toolbox, PNBODY 4.0 (Revaz 2013).

In such systems, two mechanisms are responsible for orbital decay and mass loss: tidal effects and dynamical friction induced by the dark matter halo. One way of characterizing the tidal effects on globular clusters, which induce globular cluster mass loss, is to consider the globular cluster tidal radius, defined as

$$r_t = R\left(\frac{M_{GC}}{3M_F}\right)^{1/3}, \quad (5)$$

where M_{GC} is the globular cluster mass, R is the globular cluster radial distance from the center and $M_F = M_F(D_p)$ is the Fornax mass within R_p (Binney & Tremaine 2008). In order to estimate the globular cluster mass loss, we count only bound particles. The cluster mass plays an important role in its evolution and survival. Concerning dynamical friction, which induces the orbital decay, the dynamical friction force is

$$F_{dyn} \propto \frac{\rho(r)M_{GC}^2}{V_c^2}, \quad (6)$$

where $\rho(r)$ is the Fornax density at radius r and V_c is the globular cluster circular velocity (Binney & Tremaine 2008). Theses two processes compete with and regulate each other: orbital decay increases the tidal field, which reduces the globular cluster mass, and hence slows down the orbital decay.

4.1 Physics behind our models

Here, we provide explanations concerning the dynamic behaviors of the simulations: the orbital decay and the mass loss. We are going to show that varying globular cluster mass and position can delay or accelerate these processes.

Firstly, we consider the orbital decay of the globular cluster, which is induced by dynamical friction. Since dynamical friction force is proportional to dark matter halo density, dynamical friction should be more important for LC model than WC model (see equation (7) and Figure 4). Simulations with high globular cluster mass $M_i = 8.67 \times 10^5$ M$_\odot$ illustrate this gap in Figure 5. However, mass loss reduces dynamical friction. Figure 4 shows that mass loss will be more important for LC model than SC model. Thus, it will slow down the orbital decay for LC model (see Figure 6). According to Figure 4, dynamical friction is very weak for SC model compared to the other models. All the simulations (Figures 5 and 6) show that the orbital decay is very slow for SC model.

Secondly, we consider the mass loss of the globular cluster, which depends on the enclosed mass within the globular cluster

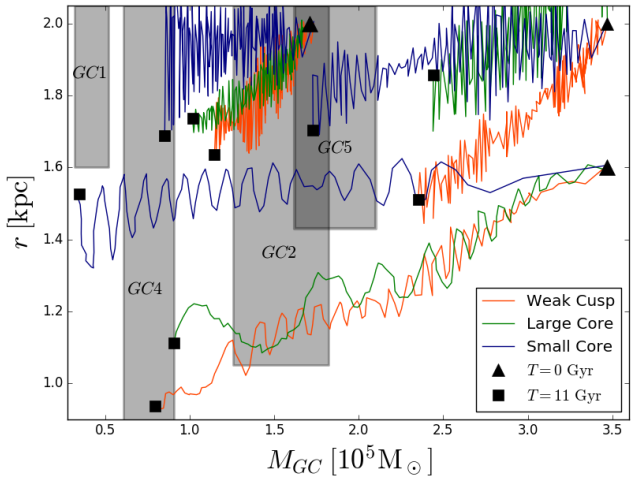

Figure 6. Globular cluster orbital decay as a function of mass loss with low initial mass $M_i = 1.71 \times 10^5$ M$_\odot$ and medium initial mass $M_i = 3.47 \times 10^5$ M$_\odot$ and a globular cluster placed at $r_i = 1.6$ and $r_i = 2$ kpc from the center for the three halo models (Weak cusp, Large Core and Small Core). All halo parameters are summarized in Table 2. The black triangles (squares) correspond to the initial $T = 0$ Gyr (final $T = 11$ Gyr) states. Final states compatible with observations, i.e. projected distance and globular cluster mass with their uncertainties, are represented by a grey area for each globular cluster. Observed data for globular clusters are summarized in Table 1.

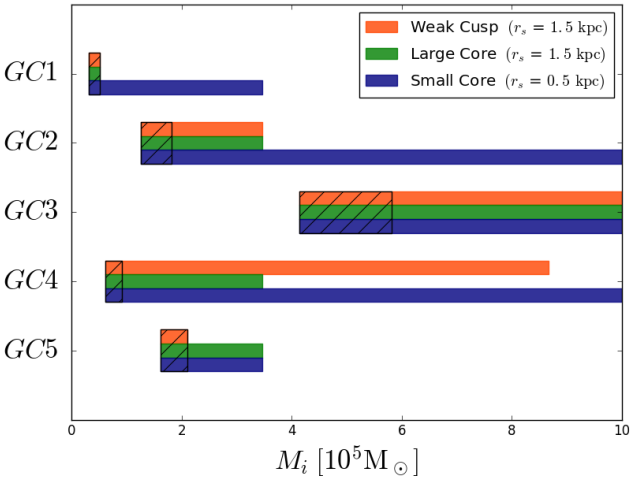

Figure 7. The range of initial globular cluster mass allowed by the three halo models (Weak cusp, Large Core and Small Core) for each globular cluster. The shaded region represents the current observed mass range for each globular cluster. This diagram summarizes all our simulation results (show in Figures 5 and 6). It is expected that the globular clusters were more massive in the past and have undergone substantial mass loss. The Small Core model is more compatible with this scenario than the other models, especially in the GC1 case. Observed data for globular clusters and halo parameters are summarized in Table 1 and Table 2.

orbit. According to Figure 4, the SC model will generate the highest mass loss. This dynamical behaviour is true for all simulations. Concerning the WC and LC models, we have to consider two cases depending on the globular cluster radius. The first one is an almost constant radial distance for the globular cluster. In this case, the LC model is going to lose more mass than the WC model (see Figure 6). The second one is a decreasing radial distance, which favors the mass loss for the WC model as we can see in Figure 6 whereas the enclosed mass is weaker for the WC model than LC model. In Figure 5, both LC and WC models lost the same amount of mass whereas their orbital decays are different. This phenomenon can be explained by the enclosed mass transition visible in Figure 4, which can correct the effect of the orbital decay on mass loss.

Oscillations of the orbital radius in all our simulations are due to particle noise. Notice that simulations with a low and medium initial cluster mass at $r_i = 2$ kpc are noisier than the others. For these initial conditions, dynamical friction is expected to be weak. There is an additional heating by particle noise, which perturbs the globular cluster dynamic. This numerical effect is more important in a lower density region.

4.2 Globular cluster started at 2 kpc with high initial mass

We ran this simulation to see whether globular clusters had high initial mass $M_i = 8.67 \times 10^5$M$_\odot$ by considering our models. According to Figure 5, high initial mass entails that the globular cluster spirals towards the center of the galaxy for all the halo models. After 11 Gyr, the final radius is $r_f < 2$ kpc. For the LC model, $r_f < D_{p_4}$, which is the smallest projected distance. In WC model, $r_f \gtrsim D_{p_3}$, whereas, in SC model, $r_f \sim D_{p_1}$, the biggest projected distance.

First, we consider the case of GC3 for each model. In all models, the final cluster mass $M_f < M_{GC3}$. To decrease the mass loss in order to be compatible with GC3 mass, we can increase the initial radius because increasing r_i will reduce mass loss and dynamical friction, that is to say increasing r_f. Hence, we establish that it is possible to find an initial radius $r_i > 2$ kpc in agreement with the spatial and mass distributions of GC3 for all models with this same high mass.

Secondly, we consider the case of the other four clusters for each model. Figure 5 shows for the three models that the mass loss is not enough to be compatible with the four globular cluster masses. Depending on M_f, all models do not work for $r_i \geqslant 2$ kpc, because increasing r_i will decrease the mass loss. However, if we want to increase mass loss, we have to decrease r_i but dynamical friction will be stronger with a lower initial radius. According to r_f, WC and LC models do not work for $r_i \leqslant 2$ kpc. However, it is possible to find $D_{p_2} < r_i < 2$ kpc in agreement with M_{GC2} and $D_{p_4} < r_i < 2$ kpc in agreement with M_{GC4} only for SC model.

To sum up, the SC model is valid for GC4, GC3 and GC2 clusters with high initial masses. Except for GC3, WC and LC models do not hold for the other globular clusters with high initial masses.

4.3 Globular cluster initially at 2 and 1.6 kpc with medium initial mass

A medium initial mass $M_i = 3.47 \times 10^5$M$_\odot$ entails that the globular cluster falls less than before for all the halo models (see Figure 6). This behaviour is predicted by equation (7). After 11 Gyr, $r_f > D_{p_1}$ for SC and LC models. In WC model, $r_f \lesssim D_{p_3}$.

According to Figure 6, the SC model meets the criteria for GC5, GC2, GC4 and GC1 with medium initial masses. For WC and LC models, the globular cluster did not lose enough mass with $r_i = 2$ kpc. To increase the mass loss, we have to decrease the initial radius. For $r_i = 1.6$ kpc, the globular cluster lost too much mass and $r_f \approx D_{p_2}$ in WC and LC models. Thus, these models work with $1.6 < r_i < 2$ kpc for GC2. In the same way, it is possible to find an initial radii $r_i < 2$ kpc in agreement with the spatial and mass distributions of GC5 for LC model according to Figure 6. Moreover,

LC and WC models are compatible with GC4, which started with initial medium mass (see Figure 6). The GC1 distributions remain a challenge for both WC and LC models.

To conclude, the SC model works for GC1, GC2, GC4 and GC5 clusters with medium initial masses. The LC model works for GC2, GC4 and GC5 with medium initial masses but the WC model is only valid for GC4 and GC2.

4.4 Globular cluster initially at 2 kpc with low initial mass

A low mass $M_i = 1.71 \times 10^5 M_\odot$ means a mass close to the observed mass. Our simulation shows that dynamical friction could not dragged a globular cluster with a low mass to the centre in any halo profiles and after 11 Gyr, $r_f > R_{p_1}$ for all models. According to Figure 6, all models work if the cluster with a low mass is far from its projected radius, that is to say $r_i > 2$ kpc in order to lose a small amount of mass over time.

The empirical results from our simulations can be summarized in Figure 7. GC1 proves to be the tightest constraint, ruling out WC and LC models. In fact, this cluster requires at the same time a weak orbital decay and a huge mass loss induced by the dark matter halo.

4.5 A constraint on the core radius

Figure 7 implies the SC model is the only one to reproduce GC5 observations for an initially more massive globular cluster. It is highly implausible that the globular clusters had initial masses close to their current masses. In this context, using the GC1 distributions, it is possible to put constraints on the core radius. Here, we consider the small core radius $r_c = 282$ pc as a reference. Increasing the core radius will increase dynamical friction and reduce the mass loss, as we can observe with the LC model (see Figure 6). However, decreasing the core radius will decrease the density and increase the enclosed mass. Then, dynamical friction effects will be weaker whereas the tidal forces will be stronger. Thus, we derive an upper limit of $r_c \lesssim 282$ pc. Based on a constraint on central phase-space density of Fornax, Strigari et al. (2006) found a upper limit of $r_c \lesssim 300$ pc, which is totally compatible with our predictions for SC model.

4.6 Implications on the nature of dark matter

The common variants on dark matter include cold dark matter (CDM), warm dark matter (WDM), fuzzy dark matter (FDM) and self-interacting dark matter (SIDM). Apart from CDM, all theses variants are apparently in favor of cored halos. We are going to discuss generic predictions of halo core radius in these theories, which are mostly based on simulations. Concerning WDM applied to Fornax, Strigari et al. (2006) established that $r_c \lesssim 85$ pc in order to avoid conservative limits from the Lyα forest power spectrum. This upper limit is compatible with our upper limit. Concerning FDM, Zhang et al. (2018) showed in general that a solitonic core with a size of 3 kpc emerges from the FDM simulation. In this simulation, the dark matter particles were ultra-light axions with a mass $O(10^{-22})$ eV. Concerning SIDM, Zavala et al. (2013) imposed that the Fornax core radius should be $r_c > 500$ pc. This estimate is based on the circular velocity of Fornax. We showed that observational data disfavor our LC model with $r_c = 848$ pc. Thus, our result favors only WDM theory if Fornax has a cored halo. The most popular candidate for WDM is the sterile neutrino. Recently, intermediate and small scale Lyman-α forest data constrains WDM candidate mass as $m_\nu > 5.3$ keV (Iršič et al. 2017). According to Tremaine & Gunn (1979), the core size of dark matter halo is related to the mass of the WDM candidate:

$$r_c \propto \frac{1}{m_\nu^2}. \quad (7)$$

For dwarf galaxies with dark matter halo masses of 10^8 (10^{10}) $M_\odot$, the core size expected for $m_\chi \approx 1$-2 keV is of the order of 20 (10) pc (Macciò et al. 2012). Thus, the WDM candidate mass lower limit induces a tiny core ($r_c < 10$ pc) for the dark matter halo.

Nevertheless, according to Hui et al. (2017), cores are required by these theories and disfavor, but do not rule out, CDM. Indeed, Pontzen & Governato (2014) claimed that it is possible to obtain a cored halo from a cuspy halo. Large clumps of gas can transfer energy to the dark matter particles via dynamical friction: the halo is quickly heated and the central cusp is flattened into a core. For Fornax, they showed that the clumps produce a central core with $r_c = 100$-300 pc in 150-200 Myr depending on the gas temperature and the clump masses (Nipoti & Binney 2015). This core radius range is totally compatible with our predictions.

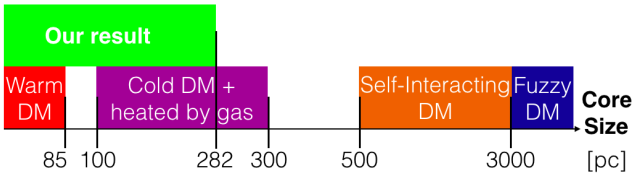

Figure 8. Constraints on the core size by dark matter theories compared to our result $r_c \lesssim 282$ pc. Our core size range is in favor of WDM theory and CDM theories, if the initial halo's central cusp is heated by gas to form a core with $r_c = 100$-300 pc in 200 Myr (Nipoti & Binney 2015).

5 CONCLUSIONS

In this work, we have revisited the cusp-core problem applied to Fornax. Currently, this dSph galaxy has five globular clusters orbiting in its dark matter halo. Observational analyses suggest that globular clusters were initially much more massive and lost most of their stars to the Fornax field. For the first time, the Fornax-globular system has been modeled with live objects, i.e. self-gravitating systems only composed of star and dark matter particles, in order to properly implement dynamical friction and tidal effects between Fornax and globular clusters. We ran pure N-body simulations for cored and cuspy halos. Based on observations and our simulations, a small cored (SC) halo ($r_c = 282$ pc) is clearly more compatible with the initially more massive globular cluster scenario than the other models (see Figure 4). We derive an upper limit of $r_c \lesssim 282$ pc. According to recent simulations for dark matter theory applied to Fornax, this core size range is only in favor of WDM theory. However, CDM theory also allows a small cored halo if the initial halo's central cusp is heated by gas to form a core with $r_c = 100$-300 pc in 200 Myr (Nipoti & Binney 2015).

The observed data disfavor the WC model, but for the moment it does not rule out a steep cusp model ($r_s = 0.1$ kpc). This model has a weaker local density and larger enclosed mass than the SC model. With our particle resolution, the heating by particle noise for these models will be very high. Increasing the simulation resolution could reduce the particle noise but employing a large number of N-body particles represents a high computational cost. In future

work, we will use our N-body code running on a GPU system (Miki & Umemura 2017) to perform simulations with very small cores.

6 ACKNOWLEDGMENTS

We thank Raphael Sadoun, Miki Yohei, Alexander Wagner, Guilhem Lavaux, Yves Revaz, Volker Springel and Carlos Carvalho for their helpful suggestions concerning simulations. We thank Pierre Salati, Simon White, Gary Mamon, Stephane Charlot and Stephane Colombi for useful conversations. We would like also to thank David Valls-Gabaud, DKR, Apolline Guillot, Simon Rozier, Amael Ellien, Valentin Decoenne, Lucas Pinol and my cats (Totem & Tabou) for their constructive suggestions to improve the manuscript. This work has made use of the Horizon Cluster hosted by Institut d'Astrophysique de Paris.

REFERENCES

Amorisco, N. C., Agnello, A., & Evans, N. W. 2013, MNRAS, 429, L89
Binney, J., & Tremaine, S. 2008, Galactic Dynamics: Second Edition, by James Binney and Scott Tremaine. ISBN 978-0-691-13026-2 (HB). Published by Princeton University Press, Princeton, NJ USA, 2008.,
Bode, P., Ostriker, J. P., & Turok, N. 2001, ApJ, 556, 93
Bullock, J. S., & Boylan-Kolchin, M. 2017, ARA&A, 55, 343
Burkert, A. 1995, ApJ, 447, L25
Chandrasekhar, S. 1943, ApJ, 97, 255
Cole, D. R., Dehnen, W., Read, J. I., & Wilkinson, M. I. 2012, MNRAS, 426, 601
Colín, P., Avila-Reese, V., & Valenzuela, O. 2000, ApJ, 542, 622
de Blok, W. J. G., McGaugh, S. S., Bosma, A., & Rubin, V. C. 2001, ApJ, 552, L23
de Boer, T. J. L., & Fraser, M. 2016, A&A, 590, A35
Dolgov, A. D., & Hansen, S. H. 2002, Astroparticle Physics, 16, 339
Fall, S. M., & Zhang, Q. 2001, ApJ, 561, 751
Fukushige, T., & Makino, J. 1997, ApJ, 477, L9
Goerdt, T., Moore, B., Read, J. I., Stadel, J., & Zemp, M. 2006, MNRAS, 368, 1073
Hernquist, L. 1990, ApJ, 356, 359
Hu, W., Barkana, R., & Gruzinov, A. 2000, Physical Review Letters, 85, 1158
Hui, L., Ostriker, J. P., Tremaine, S., & Witten, E. 2017, Phys. Rev. D, 95, 043541
Innanen, K. A., Harris, W. E., & Webbink, R. F. 1983, AJ, 88, 338
Iršič, V., Viel, M., Haehnelt, M. G., et al. 2017, Phys. Rev. D, 96, 023522
Jordán, A., McLaughlin, D. E., Côté, P., et al. 2007, ApJS, 171, 101
Larsen, S. S., Brodie, J. P., & Strader, J. 2012, A&A, 546, A53
Larsen, S. S., Strader, J., & Brodie, J. P. 2012, A&A, 544, L14
Macciò, A. V., Paduroiu, S., Anderhalden, D., Schneider, A., & Moore, B. 2012, MNRAS, 424, 1105
Mateo, M. L. 1998, ARA&A, 36, 435
Miki, Y., & Umemura, M. 2017, New Astron., 52, 65
Moore, B. 1994, Nature, 370, 629
Moore, B., Governato, F., Quinn, T., Stadel, J., & Lake, G. 1998, ApJ, 499, L5
Navarro, J. F., Frenk, C. S., & White, S. D. M. 1997, ApJ, 490, 493
Nipoti, C., & Binney, J. 2015, MNRAS, 446, 1820
Oh, K. S., Lin, D. N. C., & Richer, H. B. 2000, ApJ, 531, 727
Pontzen, A., & Governato, F. 2014, Nature, 506, 171
Read, J. I., Goerdt, T., Moore, B., et al. 2006, MNRAS, 373, 1451
Revaz, Y. 2013, Astrophysics Source Code Library, ascl:1302.004
Sadoun, R., Mohayaee, R., & Colin, J. 2014, MNRAS, 442, 160
Spekkens, K., Giovanelli, R., & Haynes, M. P. 2005, AJ, 129, 2119
Spekkens, K., Giovanelli, R., & Haynes, M. P. 2005, AJ, 129, 2119
Spergel, D. N., & Steinhardt, P. J. 2000, Physical Review Letters, 84, 3760
Springel, V. 2005, MNRAS, 364, 1105
Springel, V., Di Matteo, T., & Hernquist, L. 2005, MNRAS, 361, 776
Strigari, L. E., Bullock, J. S., Kaplinghat, M., et al. 2006, ApJ, 652, 306
Strigari, L. E., Koushiappas, S. M., Bullock, J. S., et al. 2008, ApJ, 678, 614-620
Swaters, R. A., Madore, B. F., van den Bosch, F. C., & Balcells, M. 2003, ApJ, 583, 732
Tremaine, S., & Gunn, J. E. 1979, Physical Review Letters, 42, 407
Vogelsberger, M., Zavala, J., & Loeb, A. 2012, MNRAS, 423, 3740
Walker, M. G., & Peñarrubia, J. 2011, ApJ, 742, 20
Zavala, J., Vogelsberger, M., & Walker, M. G. 2013, MNRAS, 431, L20
Zhang, J., Sming Tsai, Y.-L., Kuo, J.-L., Cheung, K., & Chu, M.-C. 2018, ApJ, 853, 51

This paper has been typeset from a TEX/LATEX file prepared by the author.